Cell Stem Cell
Article

Conversion of Mouse and Human Fibroblasts into Functional Spinal Motor Neurons

Esther Y. Son,[1,2,3,8] Justin K. Ichida,[1,2,8] Brian J. Wainger,[4,5] Jeremy S. Toma,[7] Victor F. Rafuse,[7] Clifford J. Woolf,[4,6] and Kevin Eggan[1,2,3,*]
[1]Howard Hughes Medical Institute
[2]Harvard Stem Cell Institute, Department of Stem Cell and Regenerative Biology
[3]Department of Molecular and Cellular Biology
Harvard University, Cambridge, MA 02138, USA
[4]Program in Neurobiology and FM Kirby Neurobiology Center, Children's Hospital Boston, Boston, MA 02115, USA
[5]Department of Anesthesia, Critical Care and Pain Medicine, Massachusetts General Hospital, Boston, MA 02114, USA
[6]Department of Neurobiology, Harvard Medical School, Boston, MA 02115, USA
[7]Department of Anatomy and Neurobiology, Dalhousie University, Halifax, Nova Scotia, B3H 1X5, Canada
[8]These authors contributed equally to this work
*Correspondence: keggan@scrb.harvard.edu
DOI 10.1016/j.stem.2011.07.014

SUMMARY

The mammalian nervous system comprises many distinct neuronal subtypes, each with its own phenotype and differential sensitivity to degenerative disease. Although specific neuronal types can be isolated from rodent embryos or engineered from stem cells for translational studies, transcription factor-mediated reprogramming might provide a more direct route to their generation. Here we report that the forced expression of select transcription factors is sufficient to convert mouse and human fibroblasts into induced motor neurons (iMNs). iMNs displayed a morphology, gene expression signature, electrophysiology, synaptic functionality, in vivo engraftment capacity, and sensitivity to degenerative stimuli similar to those of embryo-derived motor neurons. We show that the converting fibroblasts do not transit through a proliferative neural progenitor state, and thus form bona fide motor neurons via a route distinct from embryonic development. Our findings demonstrate that fibroblasts can be converted directly into a specific differentiated and functional neural subtype, the spinal motor neuron.

INTRODUCTION

The mammalian central nervous system (CNS) is assembled from a diverse collection of neurons, each with its own unique properties. These discrete characteristics underlie the proper integration and function of each neuron within the circuitry of the brain and spinal cord. However, their individual qualities also render particular neurons either resistant or sensitive to distinct degenerative stimuli. Thus, for each neurodegenerative disease, a stereotyped set of neuronal subtypes is destroyed, causing the hallmark presentation of that condition. Therefore, if we are to comprehend the mechanisms that underlie the development, function, and degeneration of the CNS, we must first deeply understand the properties of individual neuronal subtypes.

Physiological and biochemical studies of individual neuronal types have been greatly facilitated by the ability to isolate distinct classes of neurons and interrogate them in vitro. Most studies have focused on neurons isolated from the developing rodent CNS. However, it is not routinely possible to isolate analogous populations of human neurons or to isolate and fully study differentiated central neurons. Pluripotent stem cells, such as embryonic stem cells (ESCs), may provide an inexhaustible reservoir of diverse neural subtypes, offering an attractive approach for in vitro studies (Wichterle et al., 2002). Although stem cells have shown great promise, to date, only a handful of neural subtypes have been produced in this way. Furthermore, in many cases the neuronal populations produced from stem cells have not been shown to possess refined, subtype-specific properties, and may only superficially resemble their counterparts from the CNS (Peljto and Wichterle, 2011).

Experiments using the reprogramming of one set of differentiated cells directly into another suggest an alternative approach for the generation of precisely defined neural subtypes. Using distinct sets of transcription factors, it is possible to reprogram fibroblasts into pluripotent stem cells (Takahashi and Yamanaka, 2006), blood progenitors (Szabo et al., 2010), cardiomyocytes (Ieda et al., 2010), and functional, postmitotic neurons (Caiazzo et al., 2011; Pfisterer et al., 2011; Vierbuchen et al., 2010). We have therefore considered the idea that by using factors acting on cells intrinsically, rather than relying on morphogens that act extrinsically, it might be possible to more precisely specify the exact properties of a wide array of neuronal types. Most reprogramming studies have so far only produced induced neurons (iNs) with an unknown developmental ontogeny and a generic phenotype (Pang et al., 2011; Pfisterer et al., 2011; Vierbuchen et al., 2010). Recently, two studies have generated cells that resemble dopaminergic neurons based on the production of tyrosine hydroxylase (Caiazzo et al., 2011; Pfisterer et al., 2011). However, it is unclear whether these cells are molecularly and functionally equivalent to embryo- or ESC-derived dopaminergic neurons. In particular, it has yet to be determined whether any

type of neuron made by reprogramming can survive and properly integrate into the CNS. If neuronal reprogramming is to be successfully applied to the study of CNS function or degeneration, then it must be capable of producing specific neuronal types that possess the correct phenotypic properties both in vitro and in vivo.

To determine whether transcription factors can bestow a precise neural subtype identity, we sought factors that could reprogram fibroblasts into spinal motor neurons. Motor neurons control the contraction of muscle fibers actuating movement. Damage to motor neurons caused by either injury or disease can result in paralysis or death; consequently, there is significant interest in understanding how motor neurons regenerate after nerve injury and why they are selective targets of degeneration in diseases such as spinal muscular atrophy (SMA) and amyotrophic lateral sclerosis (ALS). We therefore attempted induction of motor neurons both because of their significant translational utility and because the developmental origins and functional properties of this neural subtype are among the most well understood.

Here we show that when mouse fibroblasts express factors previously found to induce reprogramming toward a generic neuronal phenotype (Vierbuchen et al., 2010), they also respond to components of the transcription factor network that act in the embryo to confer a motor neuron identity on committed neural progenitors. Thus, we found that forced expression of these transcription factors converted mouse fibroblasts into induced motor neurons (iMNs). Importantly, we found that the resulting iMNs had a gene expression program, electrophysiological activity, synaptic functionality, in vivo engraftment capacity, and sensitivity to disease stimuli that are all indicative of a motor neuron identity. We also show that the converting fibroblasts do not transition through a proliferative neural progenitor state before becoming motor neurons, indicating that they are formed in a manner that is distinct from embryonic development. Finally, we demonstrate that this same approach can convert human fibroblasts into motor neurons.

RESULTS

Eleven Factors Convert Fibroblasts into *Hb9::*GFP+ Cells with Neuronal Morphologies

We hypothesized that transcription factors known to instruct motor neuron formation during development might also facilitate the conversion of other cell types into motor neurons. To test this idea, we used the literature to select eight candidate transcription factors that participate in varied stages of motor neuron specification (Jessell, 2000). In order to potentially aid the transition toward a neuronal phenotype, we supplemented the motor neuron specification factors with three factors (*Ascl1*, *Brn2*, and *Myt1l*) that convert fibroblasts into iNs of a generic character (Vierbuchen et al., 2010) (Figure 1A).

For reprogramming studies, we used mouse embryonic fibroblasts (MEFs) harvested from *Hb9::*GFP mouse embryos at day E12.5, allowing spinal motor neuron conversion to be monitored. Prior to use, cultures of MEFs were carefully screened for the absence of any contaminating GFP+ cells. First, we asked whether the action of the three iN factors alone could generate *Hb9::*GFP+ cells by transducing MEFs with retroviral vectors encoding *Ascl1*, *Brn2*, and *Myt1l* (Figure 1A). Although cells with a neuronal morphology were observed, as previously reported (Vierbuchen et al., 2010), no *Hb9::*GFP+ cells emerged, even after 35 days (Figure S1A available online). This suggests that the iN factors alone do not generate motor neurons, consistent with the report that cholinergic neurons were not generated by these factors (Vierbuchen et al., 2010).

We next tested whether the eight motor neuron specification factors we selected could induce motor neurons in the absence of the three iN factors. Based on titering with a control virus encoding GFP, we determined that each factor was expressed in >95% of the fibroblasts. Encouragingly, a small number of *Hb9::*GFP+ cells were observed at 35 days posttransduction; however, they did not possess a normal neuronal morphology (Figure S1A). We therefore next asked whether the two sets of factors, iN factors and motor neuron specification factors, together could synergize to produce motor neurons. Indeed, when the aggregate set of 11 factors was transduced into fibroblasts, a significant number of *Hb9::*GFP+ cells emerged, which elaborated complex processes, and all of which expressed a neuronal form of tubulin (n = 50) (Figure 1B). We preliminarily designated these *Hb9::*GFP+ cells, iMNs.

iMNs Are Efficiently Induced by Seven Factors

To determine which of the 11 factors were necessary for generating iMNs, we omitted each gene one at a time (Figure S1B). Excluding either *Lhx3* or *Ascl1* eliminated iMN formation. However, reprogramming efficiency was either only slightly reduced or unchanged when each of the remaining factors was removed (Figure S1B). Interestingly, we observed that ectopic expression of *Hb9* was not required for iMN formation (Figure S1B), suggesting that, at least in that case, exogenous *Hb9* was not simply transactivating its own promoter. Similarly, we observed Isl1/2 expression by immunostaining in iMNs (80.6%, n = 36), even when the *Isl1* retrovirus was omitted from the transduction (Figures 1C and 1D and Figure S1B).

Although *Lhx3* and *Ascl1* seemed necessary for reprogramming, they were not sufficient to induce motor neuron formation (Figure S1C). However, when *Lhx3* was combined with the three iN factors (*Ascl1*, *Brn2*, and *Myt1l*), we observed a modest number of *Hb9::*GFP+ cells (Figure 1E). Because these four factors could not efficiently induce motor neuron formation, we next individually added each of the other factors back to this smaller set (Figure 1E). We found that either *Isl1* or *Hb9* was capable of increasing the efficiency of iMN induction, which was further enhanced when *Ngn2* was added to the other six factors (Figure 1F). Indeed, the efficiency of motor neuron induction with these seven factors (*Ascl1*, *Brn2*, *Myt1l*, *Lhx3*, *Hb9*, *Isl1*, and *Ngn2*) surpassed the activity of the 11 as a whole and, depending on the culture conditions used, reached between 5% and 10% of the number of MEFs transduced (Figure 1F and Figure S1E). Adding any one of the remaining factors, which are all known to function in earlier stages of motor neuron specification (Lee et al., 2005), dramatically decreased the efficiency of reprogramming by the seven factors (Figure S1D).

We reasoned that, although our apparently homogeneous MEF cultures lacked *Hb9::*GFP+ cells, they could be contaminated with rare embryonic neuronal progenitors that might be more responsive to reprogramming. To rule out the possibility that iMNs originated from such progenitors, we prepared

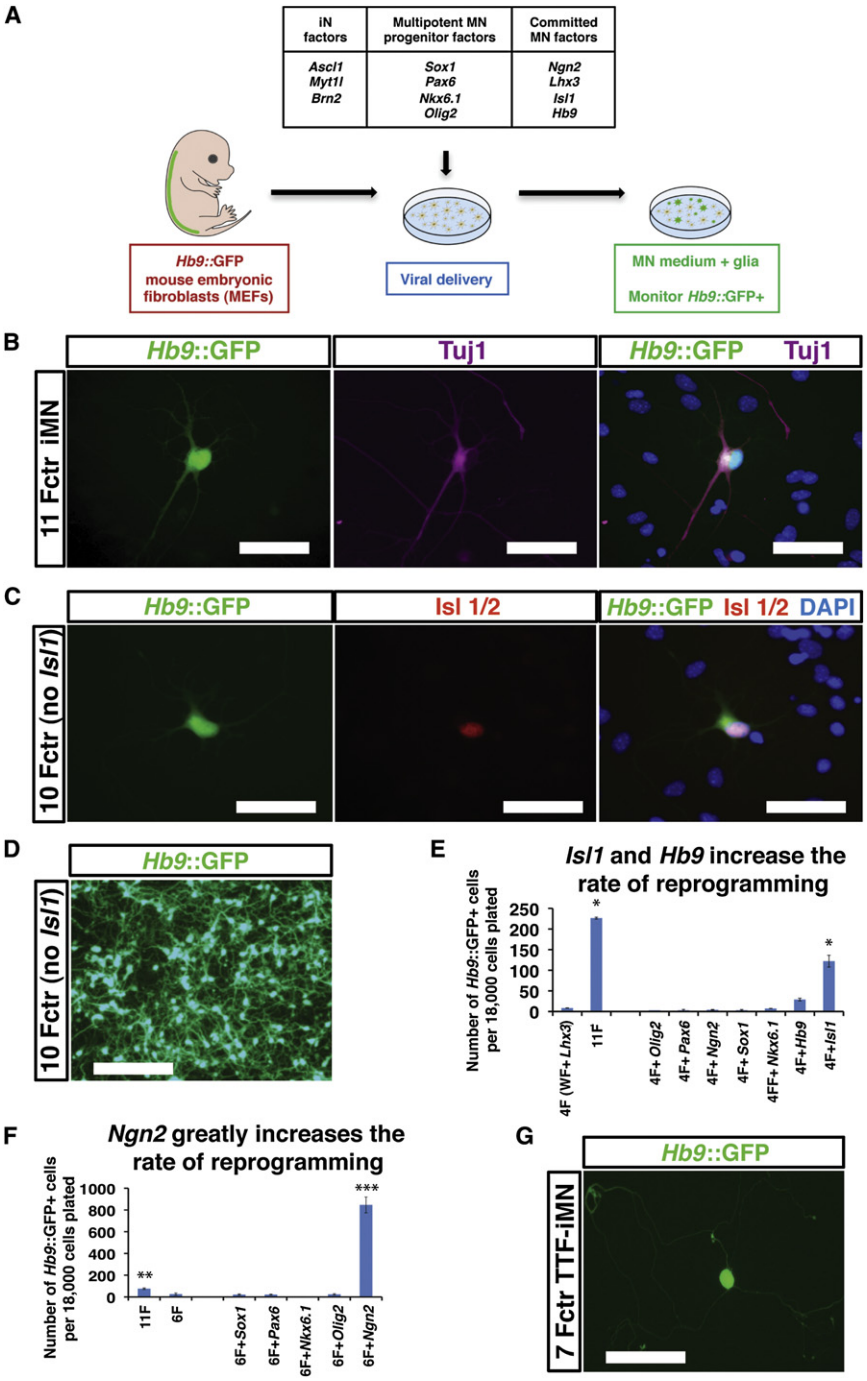

Figure 1. Generation of *Hb9::*GFP+ iMNs by Seven Factors

(A) Experimental outline. Eleven candidate transcription factors include eight developmental genes in addition to the three iN factors.

(B) *Hb9::*GFP+ neurons express Tuj1 (purple). Scale bars represent 40 μm.

(C) iMNs generated with 10 factors (without *Isl1*) express endogenous Islet (red). Scale bars represent 40 μm.

(D) *Isl1* is dispensable for generating iMNs. Scale bar represents 200 μm.

(E) Reprogramming efficiency is greater with *Hb9* or *Isl1* on top of four factors (*Lhx3*, *Ascl1*, *Brn2*, and *Myt1l*) at day 21 posttransduction. Error bars indicate ± SD. *$p < 0.05$ (Student's t test, two-tailed).

(F) Addition of *Ngn2* to the six-factor pool (*Hb9*, *Isl1*, *Lhx3*, *Ascl1*, *Brn2*, and *Myt1l*) greatly enhances reprogramming efficiency as seen 10 days after transduction. Error bars indicate ± SD. ***$p < 0.001$; **$p < 0.01$ (Student's t test, two-tailed).

(G) The seven iMN factors convert adult tail tip fibroblasts into motor neurons. Scale bar represents 100 μm.

See also Figure S1.

fibroblasts from the tails of adult *Hb9::*GFP mice and transduced them with the optimal set of seven factors. Again, GFP+ cells with neuronal morphologies emerged (Figure 1G), indicating that the ability to respond to the seven iMN factors was not restricted to cells of an embryonic origin.

iMNs Possess a Motor Neuron Gene Expression Signature

To begin to assess whether iMNs had the known characteristics of cultured embryonic motor neurons, we carefully examined the phenotype of iMNs made with 10 factors (*Isl1* omitted). We found that iMNs were comparable in cell body size and projection length to both E13.5 embryo- and ESC-derived motor neuron controls (Figure S2A). To determine how similar overall transcription in iMNs was to control motor neurons, we isolated the three motor neuron types by fluorescence-activated cell sorting (FACS) and performed transcriptional profiling (Figures 2A–2D). For these analyses, RNAs isolated from MEFs and ESCs were used as negative controls. When we performed hierarchical clustering of the data, iMNs grouped closely to embryonic motor neurons, as did ESC-derived motor neurons (Figure 2A). In contrast, iMNs were very distinct from the initial MEF population. Thus, our results suggest that transduction of MEFs with these transcription factors results in a global shift toward a motor neuron transcriptional program.

When we examined the transcription of specific neuronal genes, we again found that iMNs and control motor neurons were very similar. Relative to either MEFs or ESCs, iMNs and both types of control motor neurons expressed elevated levels of β2-tubulins (*Tubb2a* and *Tubb2b*) and *Map2* (Figures 2B–2D and Figure S2B), as well as synaptic components such as synapsins (*Syn1* and *Syn2*), synaptophysin (*Syp*), and synaptotagmins (*Syt1*, *Syt4*, *Syt13*, and *Syt16*) (Figures 2B–2D and Figure S2C). iMNs also expressed known motor neuron transcription factors that were not provided exogenously (*Neurod1*

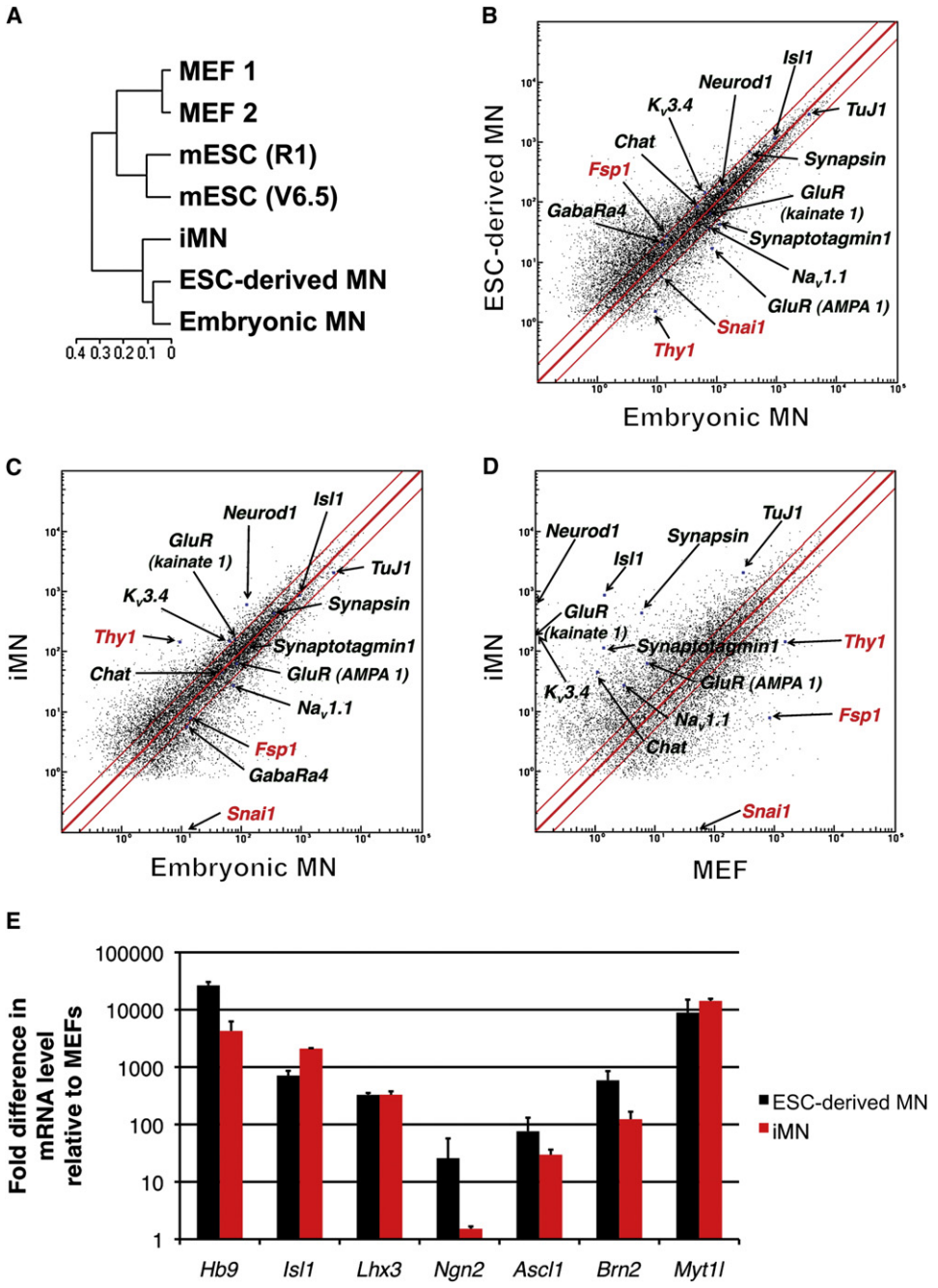

Figure 2. iMNs Possess Gene Expression Signatures of Motor Neurons

(A) Global transcriptional analysis of FACS-purified *Hb9::*GFP+ motor neurons. iMNs cluster with control motor neurons, away from MEFs.

(B–D) Pairwise gene expression comparisons show that iMNs are highly similar to embryo-derived motor neurons and dissimilar from the starting MEFs; black labeling denotes genes expressed in motor neurons, red labeling denotes genes expressed in fibroblasts, and the red lines indicate the diagonal and 2-fold changes between the sample pairs.

(E) qRT-PCR data showing expression of endogenous transcripts of the seven iMN factors in iMNs and in ESC-derived motor neurons, relative to their levels in MEFs. Error bars indicate ± SD.

See also Figure S2 and Table S1.

and *Isl1*) (Figures 2C and 2D and Figure S2D), as well as the gene encoding the enzyme cholineacetyltransferase (*Chat*) (Figures 2C and 2D and Figure S2E). In contrast, iMNs had downregulated the fibroblast program as exemplified by reduced transcription *of Snai1*, *Thy1*, and *Fsp1* (Figure 2D and Figure S2F). Immunostaining confirmed that the iMNs expressed Map2

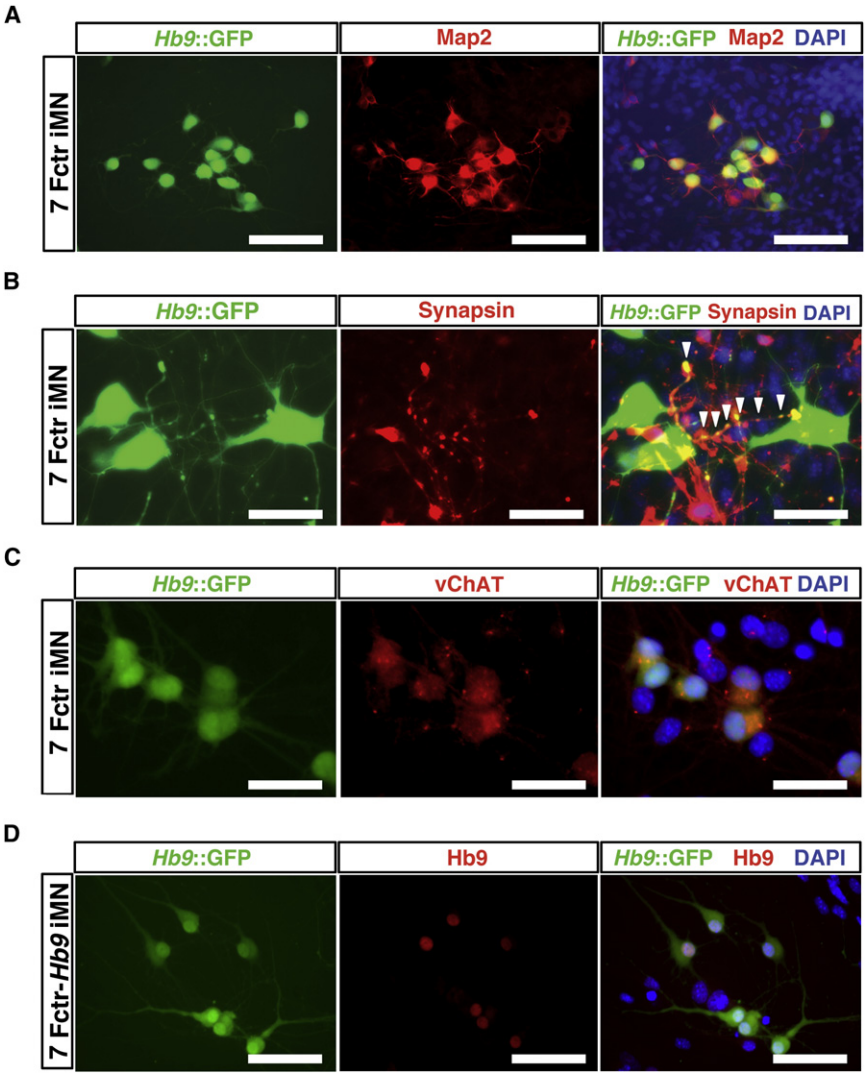

Figure 3. iMNs Express Neuronal and Motor Neuron Proteins

(A) iMNs express the panneuronal marker Map2 (red). Scale bars represent 100 μm.

(B) iMNs express synapsin (red). Scale bars represent 20 μm.

(C) iMNs express vesicular cholineacetyltransferase (vChAT, red). Scale bars represent 40 μm.

(D) iMNs express the motor neuron-selective transcription factor Hb9 (red). Scale bars represent 80 μm.

See also Figure S2.

(100%, n = 120) (Figure 3A), synapsin (Figure 3B), and vesicular ChAT (97.6%, n = 124) (Figure 3C), indicating that they had indeed activated the enzymatic pathways for producing acetylcholine (ACh), the neurotransmitter released by motor neurons, and suggesting they should be capable of forming functional synapses. In contrast, the vast majority of iMNs did not express tyrosine hydroxylase (97%, n = 150) (Figure S2G), suggesting that they were not of a mixed neuronal character.

In order to determine if the iMNs truly adopted a new cellular identity through transdifferentiation, we performed qRT-PCR analysis to ask if they established an endogenous program of motor neuron gene expression (Table S1, available online). As expected for a somatic cell type such as the motor neuron, the retroviral transgenes used for reprogramming were not silenced in the iMNs (Figure S2H), leaving it unclear as to whether the endogenous loci of these motor neuron genes had been activated. When we quantified the endogenous mRNA levels of the motor neuron-specific genes used for conversion, we found that all seven transcription factors were expressed at levels similar to those in ESC-derived motor neurons (Figure 2E). Furthermore, immunostaining revealed that iMNs created without exogenous Hb9 still activated expression of this important transcription factor from the endogenous locus (87.9%, n = 149) (Figure 3D). Together, these data indicate that the iMNs we produced had established a transcriptional program characteristic of motor neurons.

iMNs Possess the Electrophysiological Characteristics of Motor Neurons

In order to determine if MEF- and tail tip fibroblast-derived iMNs possessed the electrophysiological properties of motor neurons, we performed whole-cell patch-clamp recordings. The average resting membrane potential for iMNs was −49.5 mV (SEM = 5.6, n = 6), which was similar to that for control ESC-derived motor neurons (−50.5 mV, SEM = 3.5, n = 13). Depolarizing voltage steps in voltage-clamp mode elicited fast inward currents followed by slow outward currents, consistent with the opening of voltage-activated sodium and potassium channels, respectively (Figures 4A and 4B and Figure S3A). The inward current was blocked by addition of 500 nM tetrodotoxin (TTX), a potent antagonist of TTX-sensitive voltage-activated sodium channels (Figure 4C). A defining feature of a neuron is its ability to fire action potentials. In current-clamp experiments with iMNs, depolarizing current steps produced single or multiple action potentials (90%, n = 10), with overshoot, afterhyperpolarizations, and a firing frequency similar to that reported for ESC-derived motor neurons and rat embryonic motor neurons (Alessandri-Haber et al., 1999) (Figures 4D and 4E and Figure S3B).

We next tested whether iMNs express functional receptors for the excitatory and inhibitory neurotransmitters that normally act on motor neurons. As might be expected given the known receptor subunit transitions associated with development of immature neurons to a fully differentiated state, certain agonists yielded responses in some, but not all, neurons. Glycine and GABA are the major inhibitory neurotransmitters, and their ionotropic activity is mediated by opening chloride channels.

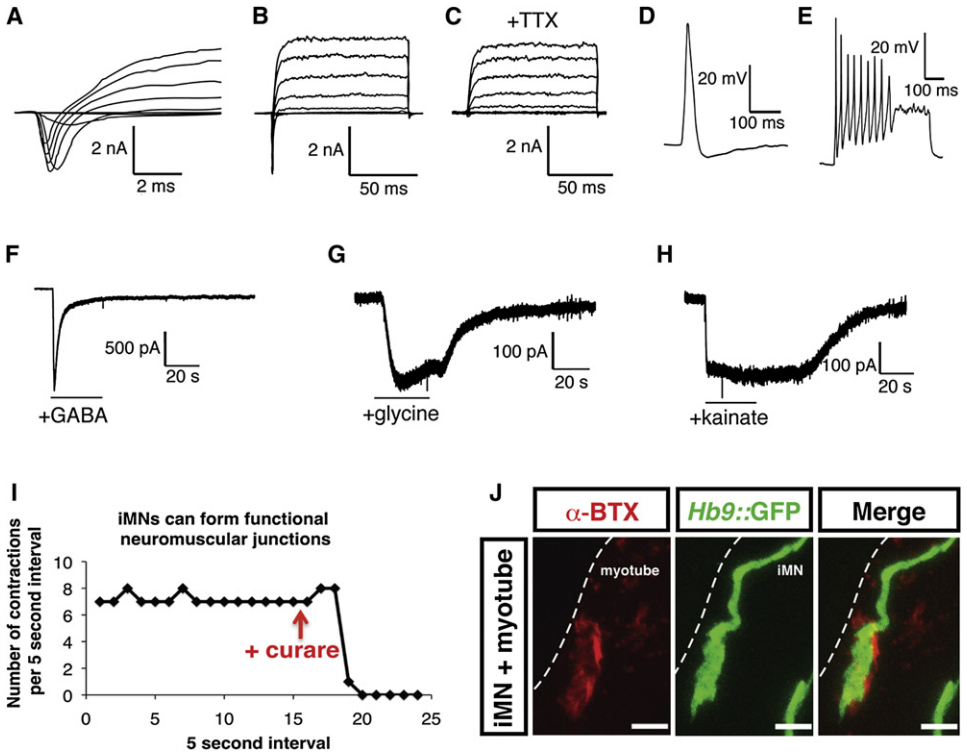

Figure 4. Electrophysiological Activity and In Vitro Functionality of iMNs

(A) iMNs express functional sodium channels.

(B) iMNs express functional sodium and potassium channels.

(C) iMN sodium channel activity is appropriately blocked by tetrodotoxin (TTX).

(D) iMNs fire a single action potential upon depolarization.

(E) iMNs fire multiple action potentials upon depolarization.

(F) 100 μM GABA induces inward currents in iMNs.

(G) 100 μM glycine induces inward currents in iMNs.

(H) 100 μM kainate induces inward currents in iMNs.

(I) iMN-induced contractions of C2C12 myotubes are blocked by 50 μM curare. The arrow indicates the timing of curare addition.

(J) iMNs cultured with chick myotubes form NMJs with characteristic α-bungarotoxin (α-BTX, red) staining. The dotted line outlines the boundaries of a myotube. Scale bar represents 5 μm.

See also Figure S3, Table S2, and Movie S1.

Addition of 100 μM glycine (44.4%, n = 9, Figure 4G) or GABA (72.7%, n = 11, Figure 4F, and Figure S3C) elicited inward currents when cells were held at −80 mV. We also evaluated the response of iMNs to fast excitatory glutamatergic neurotransmitters and observed a strong response to the receptor agonist kainate (80%, n = 15 cells, Figure 4H, and Figure S3D).

Consistent with our physiological analyses, and similar to control embryonic motor neurons and motor neuron populations described previously (Cui et al., 2006), the iMNs transcribed the genes encoding α and β subunits of voltage-gated sodium channels (Figures 2C and 2D and Figure S3E) as well as members of the Shaker-, Shaw-, and Eag-related, inwardly rectifying, and calcium-activated families of potassium channels (Figures 2C and 2D and Figure S3G). In addition, iMNs transcribed genes encoding the receptor components required for responding to the neurotransmitter glutamate (Figures 2C and 2D and Figure S3F). Together, our physiological and gene expression analyses indicate that iMNs are excitable, generate action potentials, and respond to both inhibitory and excitatory neurotransmitters in a manner characteristic of both ESC-derived and embryonic motor neurons.

iMNs Form Functional Synapses with Muscle

Our initial results indicated that iMNs have many of the phenotypic and electrophysiological properties of bona fide motor neurons. However, the defining functional characteristic of the spinal motor neuron is its ability to synapse with muscle and, through the release of ACh, stimulate muscle contraction. To test whether iMNs could form functional neuromuscular junctions (NMJs), we cocultured FACS-purified iMNs with myotubes derived from the C2C12 muscle cell line. We found that iMNs could establish themselves in these muscle cultures and sent projections along the length of the myotubes (Figure S3H).

Strikingly, we observed that several days following the addition of purified iMNs, C2C12 myotubes began to undergo regular and rhythmic contraction (Figure 4I). Regular contractions were not seen at this time point in myotubes that were cultured alone or with generic iNs (Table S2). To directly test

whether the regular contractions of mytotubes were due to synaptic stimulation of ACh receptors, we quantified the frequency of myotube contraction and then added curare to the culture medium. Because curare selectively and competitively antagonizes nicotinic ACh receptors, its addition should only inhibit muscle contractions that result from stimulation of such receptors (Figure 4I and Movie S1 available online). Shortly after the addition of curare, we observed a precipitous and sustained decline in the frequency of myotube contraction, indicating that the contractions were indeed dependent on the stimulation of ACh receptors.

In order to directly visualize NMJ formation in iMN cultures, we cocultured iMNs with primary chick myotubes (Figure 4J and Figures S3I–S3L). After 1 week of coculture, we found that many *Hb9::*GFP+ iMNs survived even following withdrawal of neurotrophic support, suggesting that they had formed synapses with the muscle. Three weeks after coculture had been initiated, staining with α-bungarotoxin (α-BTX) revealed ACh receptor clustering on the myofibers (Figures 4J and Figures S3I–S3K). As occurs in ESC-derived motoneuron/chick myotube cocultures (Miles et al., 2004; Soundararajan et al., 2007), ACh receptors clustered preferentially near the iMN axons, although the clustering was not always clearly opposed to *Hb9::*GFP+ axons. This phenomenon is similar to what occurs during chick (Dahm and Landmesser, 1988) and mouse (Lupa and Hall, 1989) neuromuscular development, where receptor clustering first appears near the innervating motor axons, but not always in direct contact. Imaging in the x-z and y-z orthogonal planes verified that ACh receptors clustered near iMN axons superimposed with the *Hb9::*GFP+ axons (Figure S3L). These results indicate that iMNs signal to the postsynaptic muscle fiber to induce appropriate receptor clustering, which is necessary for neuromuscular transmission. Together, these data indicate that iMNs can make functional synaptic junctions with muscle.

iMNs Integrate into the Developing Chick Spinal Cord

Transplantation of motor neurons into the developing chick spinal cord provides a rigorous test of their ability to survive in vivo, migrate to appropriate engraftment sites in the ventral region of the spinal cord, and properly respond to axon guidance cues to send their axonal projections out of the spinal cord through the ventral root (Peljto et al., 2010; Soundararajan et al., 2006; Wichterle et al., 2002). In order to test the ability of iMNs to survive and function in vivo, we transplanted FACS-purified iMNs or control ESC-derived motor neurons into the neural tube of stage 17 chick embryos at 12–16 days posttransduction (Figure 5A). Although the injection of the iMNs along the dorsal-ventral axis was not precisely controlled, we observed that *Hb9::*GFP+ iMNs engrafted in the ventral horn of the spinal cord in the location where endogenous motor neurons reside at stage 31 (Figure 5B). Like transplanted ESC-derived motor neurons (Soundararajan et al., 2006; Wichterle et al., 2002), the *Hb9::*GFP+ cells maintained Tuj1 expression and exhibited extensive dendritic arbors (Figure 5B). In addition, we asked whether iMNs project their axons out of the CNS. Endogenous and transplanted ESC-derived motor neurons send axonal projections out of the spinal cord through the ventral root toward musculature (Figure S4) (Soundararajan et al., 2010; Wichterle et al., 2002). When *Hb9::*GFP ESCs are subjected to directed differentiation toward motor neurons, the resulting EBs contain both GFP+ motor neurons and distinct, nonmotor neuronal subtypes that do not express GFP. In contrast to GFP+ motor neurons, GFP− nonmotor neuron subtypes present within the same transplants extend extensive processes whose projections remain restricted to the developing spinal cord and do not exit through the ventral root (Soundararajan et al., 2010). Therefore, the chick transplantation assay can be used to measure motor neuron-specific axonal pathfinding. Indeed, after transplantation, we often observed *Hb9::*GFP+ iMNs in the ventral horn of the spinal cord, and in 80% (n = 5) of these cases, we saw axons of *Hb9::*GFP+ iMNs projecting out of the spinal cord through the ventral root toward the musculature (Figure 5B). Thus, their in vivo engraftment capacity was similar to that observed for ESC-derived *Hb9::*GFP+ motor neurons (Figure S4). Together, these data demonstrate that iMNs are able to engraft, migrate to appropriate sites of integration, and correctly respond to guidance cues in vivo, projecting their axons out of the CNS.

iMNs Are Sensitive to Disease Stimuli

ALS is an invariably fatal neurological condition whose hallmark is the selective and relentless degeneration of motor neurons. We reasoned that if iMNs fully phenocopied bona fide motor neurons, they should also be sensitive to degenerative stimuli thought to contribute to ALS. To determine if this were the case, we cocultured iMNs with glial cells from the *SOD1*G93A mouse model of ALS. We, and others, have shown that both embryonic and ESC-derived motor neurons are selectively sensitive to the toxic effect of mutant glia, while other neural cell types, such as spinal interneurons, are relatively unaffected (Di Giorgio et al., 2007) (Nagai et al., 2007). iMNs were cocultured with either wild-type or mutant *SOD1*G93A glia and the number of *Hb9::*GFP+ iMNs was quantified 10 days later. As we would expect if iMNs were indeed bona fide motor neurons, there was a sharp reduction in the number of iMNs cocultured with mutant glia relative to those cultured with wild-type glia (Figures 5C and 5D), and the effect was similar in magnitude to its reported effect on ESC-derived motor neurons (Di Giorgio et al., 2007) (Nagai et al., 2007).

Currently, it is unclear whether there are cell-autonomous mechanisms of motor neuron degeneration induced by mutant SOD1 that can lead to overt differences in motor neuron survival in vitro. To see whether iMNs could be used to answer this question, we asked if there is a survival difference between wild-type and *SOD1*G93A iMNs in culture with wild-type glia. We prepared MEFs from mouse embryos that overexpress the *SOD1*G93A transgene as well as harbor the *Hb9::*GFP reporter, and transdifferentiated them into *Hb9::*GFP+ iMNs alongside MEFs that only contain the *Hb9::*GFP reporter. We then FACS-purified *Hb9::*GFP+ iMNs of both genotypes in parallel and plated the same number of cells for each on wild-type glia. After 4 days in culture, we observed impaired survival of *SOD1*G93A iMNs relative to control iMNs (Figure 5E), suggestive of a cell-autonomous disease phenotype. Taken together, these results indicate that iMNs are useful for studying both cell-autonomous and non-cell-autonomous contributors to motor neuron degeneration in ALS.

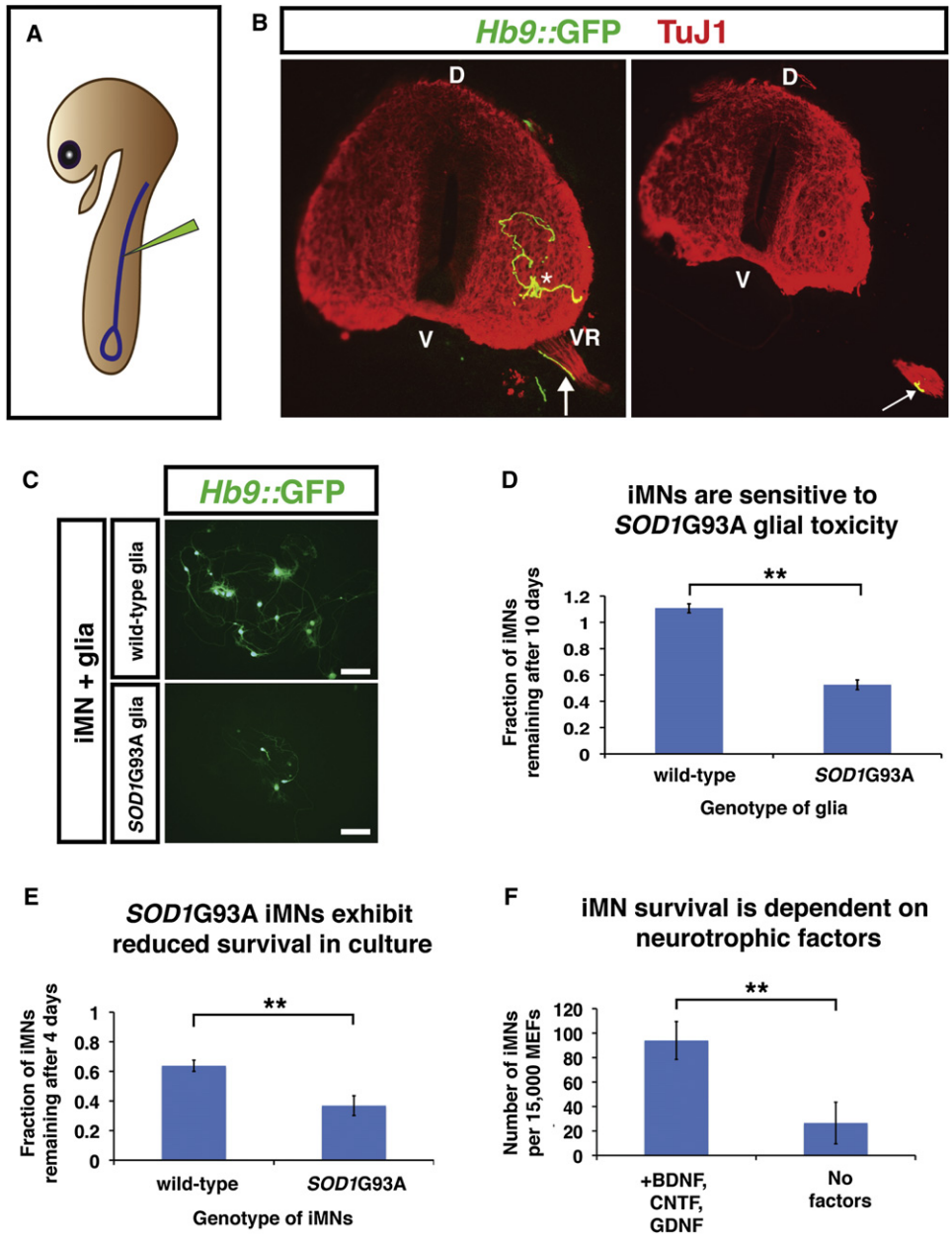

Figure 5. In Vivo Functionality and In Vitro Utility of iMNs

(A) Diagram showing the injection of iMNs into the neural tube of the stage 17 chick embryo.

(B) Transverse sections of iMN-injected chick neural tube 5 days after transplantation. Arrows in both panels indicate the same axon of an iMN exiting the spinal cord through the ventral root. D: dorsal, V: ventral, VR: ventral root.

(C) FACS-purified *Hb9::*GFP+ iMNs cocultured with wild-type or the mutant *SOD1*G93A-overexpressing glia for 10 days. Scale bars represent 5 μm.

(D) Quantification of (C). Error bars indicate ± SD. **p < 0.01 (Student's t test, two-tailed).

(E) *SOD1*G93A iMNs exhibit reduced survival in culture with wild-type glia. Error bars indicate ± SD. **p < 0.01 (Student's t test, two-tailed).

(F) Changes in iMN number after 9 days of culture in the presence or absence of neurotrophic factors (GDNF, BDNF, and CNTF). Error bars indicate ± SD. **p < 0.01 (Student's t test, two-tailed).

See also Figure S4.

Because there is significant interest in the identity of factors and pathways that modulate neuronal survival in the context of neurodegenerative diseases, we also tested whether iMNs were similar to motor neurons in their sensitivity to growth factor withdrawal. Indeed, when the neurotrophic factors GDNF, BDNF, and CNTF were all withdrawn from the medium, iMNs were lost more rapidly (Figure 5F). Thus, iMNs share a neurotrophic support requirement similar to embryonic motor neurons, and we conclude that iMNs could serve as a suitable substrate for in vitro studies of motor neuron function, disease, and injury.

Fibroblasts Do Not Transit through a Neural Progenitor State before Becoming iMNs

The process by which the initial fibroblasts undergo conversion into another cell type in defined-factor reprogramming and transdifferentiation experiments remains poorly understood. In particular, it is currently unknown if the somatic cells reprogram through the same developmental intermediates that are found in the developing embryo, for example, by first dedifferentiating and then redifferentiating through a neural progenitor state into a neuron, or if they instead convert more "directly." To address this question, we used a lineage tracing approach to ask if, during the course of reprogramming, a gene commonly used to identify neuronal progenitors ever became expressed.

Motor neuron progenitor cells are highly proliferative in culture (Frederiksen and McKay, 1988; Jessell, 2000). To determine whether iMNs transited through a highly proliferative intermediate during the reprogramming process, we quantified the timing of cell division in the reprogramming cultures using 48 hr pulses of BrdU. Following transduction, we found that the cells incorporated decreasing amounts of BrdU at each subsequent time point and did not incorporate detectable levels of BrdU after 4 days post-transduction (Figure 6A). Consistent with a previous report (Vierbuchen et al., 2010), these results suggest that the transduced cells quickly become postmitotic. Since 10% of the fibroblasts eventually become iMNs, and because GFP+ iMNs do not begin to appear in culture until day 5 and the majority arise between 7 and 14 days in culture, these results suggest that the iMNs are not being produced from highly proliferative neuronal progrenitors.

To more definitively test if the fibroblasts become motor neuron progenitors before differentiating into iMNs, we repeated the induction of a motor neuron identity using transgenic fibroblasts with a *Nestin*::CreER (Burns et al., 2007); LOX-STOP-LOX-H2B-mCherry (Abe et al., 2011); *Hb9*::GFP genotype (Figure 6B). Because Nestin is a well-known marker of neural progenitor cells in the mammalian CNS (Messam et al., 2002), we reasoned that if the fibroblasts transited through a progenitor state before becoming motor neurons, the resulting iMNs would activate expression of *Nestin::*CreER, recombine the reporter gene, and thus express both mCherry and *Hb9::*GFP.

First, as a positive control for this experiment, we generated induced pluripotent stem cells (iPSCs) from the fibroblasts, then used retinoic acid and Sonic Hedgehog (Wichterle et al., 2002) to differentiate the iPSCs into motor neurons. Because this directed differentiation protocol mimics development, we expected the resulting motor neurons to originate from Nestin+ precursors. When we performed the differentiation without 4-hydroxytamoxifen (4-OHT), none of the resulting *Hb9*::GFP+ motor neurons expressed mCherry (Figure 6C). However, when we added 4-OHT to the differentiation, 3% of the motor neurons coexpressed mCherry ($n > 2,000$) (Figure 6C), verifying that the *Nestin*::CreER reporter successfully identified motor neurons that transited through a Nestin+ progenitor state. In contrast, when we treated the seven factor-transduced MEF cultures with 4-OHT both before and during transdifferentiation, none of the resulting iMNs expressed mCherry ($n > 5,000$) (Figure 6D). These results confirm that fibroblasts do not become iMNs by transiting through a motor neuron progenitor cell state, and further rule out the possibility that many of the iMNs are derived from contaminating neural progenitor cells in the MEF cultures.

Human iMNs Can Be Generated by Eight Transcription Factors

We next sought to determine whether the same or a similar set of factors could be used to generate human iMNs from fibroblasts. To this end, human embryonic fibroblasts (HEFs) were derived from a human ESC line harboring the *Hb9::*GFP transgene (Di Giorgio et al., 2008). The HEFs were then transduced with viruses containing the seven iMN factors identified in the mouse system as well as *NEUROD1*, a proneural gene reported to enhance the conversion efficiency of human fibroblasts into iNs (Pang et al., 2011). Thirty days after transduction, we observed *Hb9::*GFP+ cells with highly neuronal morphologies in the culture of eight factor-transduced HEFs (Figures 7A and 7B), whereas untransduced HEFs never spontaneously expressed the transgene under the same conditions (Figure 7B). These putative human iMNs expressed vesicular ChAT (Figure 7C), indicating that they were indeed cholinergic in nature.

In order to assess the functionality of human iMNs made with eight factors, we employed whole-cell patch-clamp recording to look at their electrophysiological properties. Similar to their mouse counterparts, human iMNs expressed functional voltage-gated sodium and potassium channels (Figure 7D) and were able to fire action potentials (Figure 7E) when depolarized. Importantly, they responded appropriately to the addition of 100 μM kainate (Figure 7F) and 100 μM GABA (Figure 7G), demonstrating their ability to receive and respond to the major excitatory and inhibitory inputs, respectively, that govern spinal motor neuron activity. Therefore, functional iMNs can be generated from human fibroblasts by transdifferentiation.

DISCUSSION

We have shown that a small set of transcription factors can convert embryonic and adult fibroblasts into functional motor neurons. The iMNs expressed panneuronal and motor neuron-specific markers, as well as the receptors and channels that generate excitable membranes sensitive to transmitters, allowing them to both fire action potentials and receive synaptic input. These cholinergic iMNs also possessed the defining hallmark of motor neurons: the ability to synapse with muscle and to induce its contraction. Most importantly, iMNs are able to contribute to the developing CNS in vivo, migrating appropriately to the ventral horn and sending out axonal projections through the ventral root. We also demonstrated that the iMNs are sensitive to a degenerative ALS stimulus that selectively affects motor neurons. Thus we provide several lines of evidence that iMNs are functional motor neurons with consequent utility for the study of motor neuron physiology and disease susceptibility.

It is critical to note that we cannot rule out the possibility that other motor neuron-inducing factors have been overlooked, or that varying the cocktail of genetic factors might further enhance the frequency or even accuracy of conversion. In addition, it will be important to determine whether the factors we have identified here, or a group of similar factors, can efficiently convert adult human fibroblasts into motor neurons. Such a reprogramming approach would greatly facilitate the production of patient-specific motor neurons for therapeutic uses in regenerative medicine and for disease-related studies.

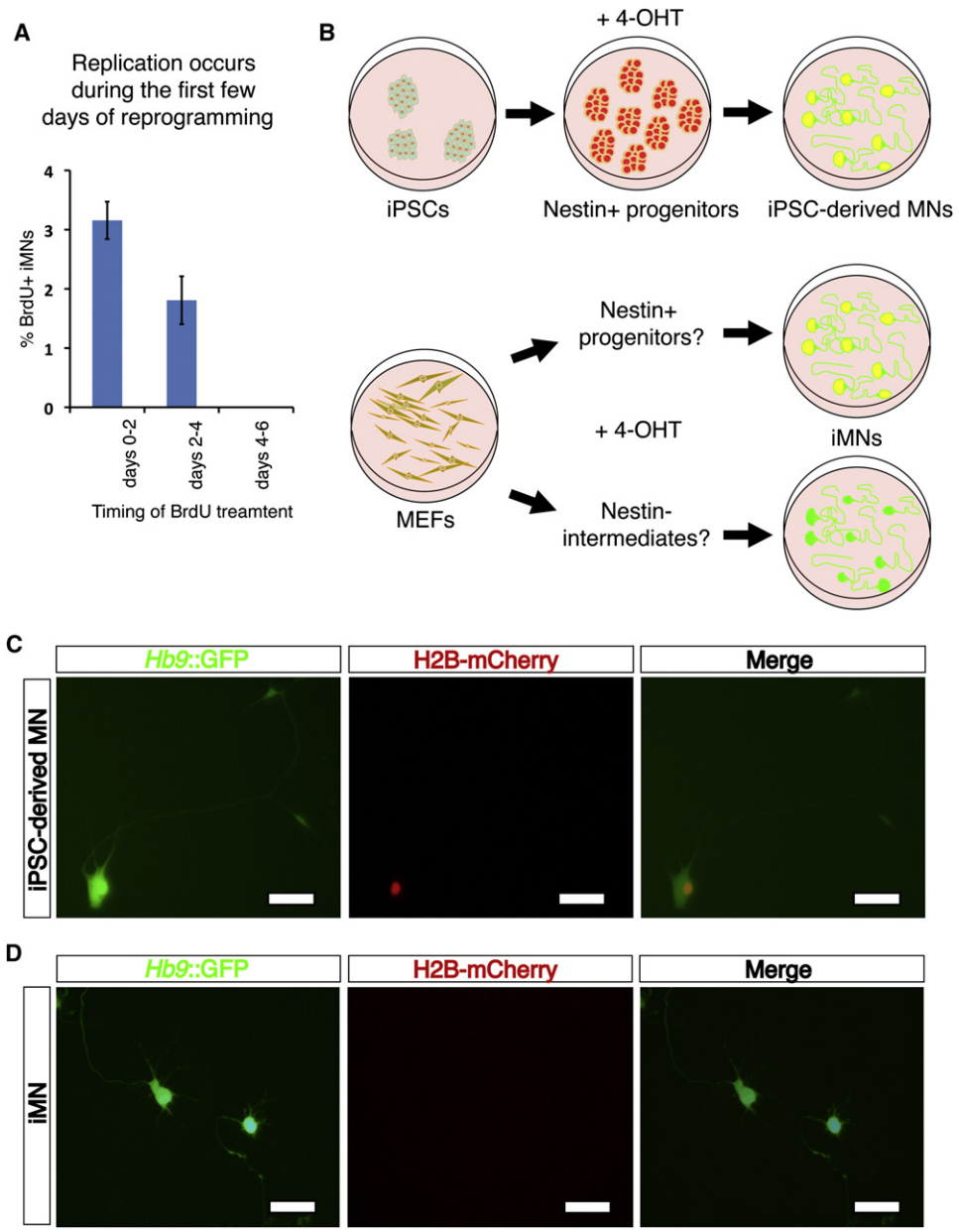

Figure 6. Transdifferentiation Does Not Occur through a Nestin+ Neural Progenitor State

(A) Percentage of iMNs that have incorporated BrdU. Error bars indicate ± SD.

(B) Outline of the lineage tracing experiment using *Nestin::*CreER; LOX-STOP-LOX-H2B-mCherry; *Hb9::*GFP iPSCs or MEFs. To detect Nestin+ intermediates, cultures were treated with 1–2 μM 4-OHT during directed differentiation of iPSCs (positive control) or during transdifferentiation of fibroblasts by the seven factors.

(C) FACS-purified, mCherry+ *Hb9::*GFP+ motor neurons derived from the triple transgenic iPSCs in the presence of 1 μM 4-OHT. Expression of mCherry was observed in 3% of *Hb9::*GFP+ cells (n > 2,000) and indicates the activation of *Nestin::*CreER during directed differentiation. Scale bars represent 40 μm.

(D) mCherry− *Hb9::*GFP+ iMNs generated from the triple transgenic MEFs by transdifferentiation in the presence of 2 μM 4-OHT. mCherry+ iMNs were never observed (n > 5,000), suggesting that a Nestin+ state is not accessed during reprogramming. Scale bars represent 40 μm.

It is remarkable that the conversion to motor neurons occurs so efficiently given that the cells do not transit through a neural progenitor state. It was striking that under certain conditions, as many as one *Hb9::*GFP+ iMN was made from every 10 MEFs. This efficiency was substantially higher than iPSC reprogramming (Takahashi and Yamanaka, 2006) and could be the result of a cooperative process in which establishment of a general neuronal program is augmented by specific patterning to a motor neuron identity. These results indicate that the massive changes in gene expression induced during defined-factor reprogramming can be executed efficiently even though they do not mimic embryonic development precisely. In the future it will be of interest to determine whether this approach can serve as a general strategy for the production of many distinct neuronal subtypes.

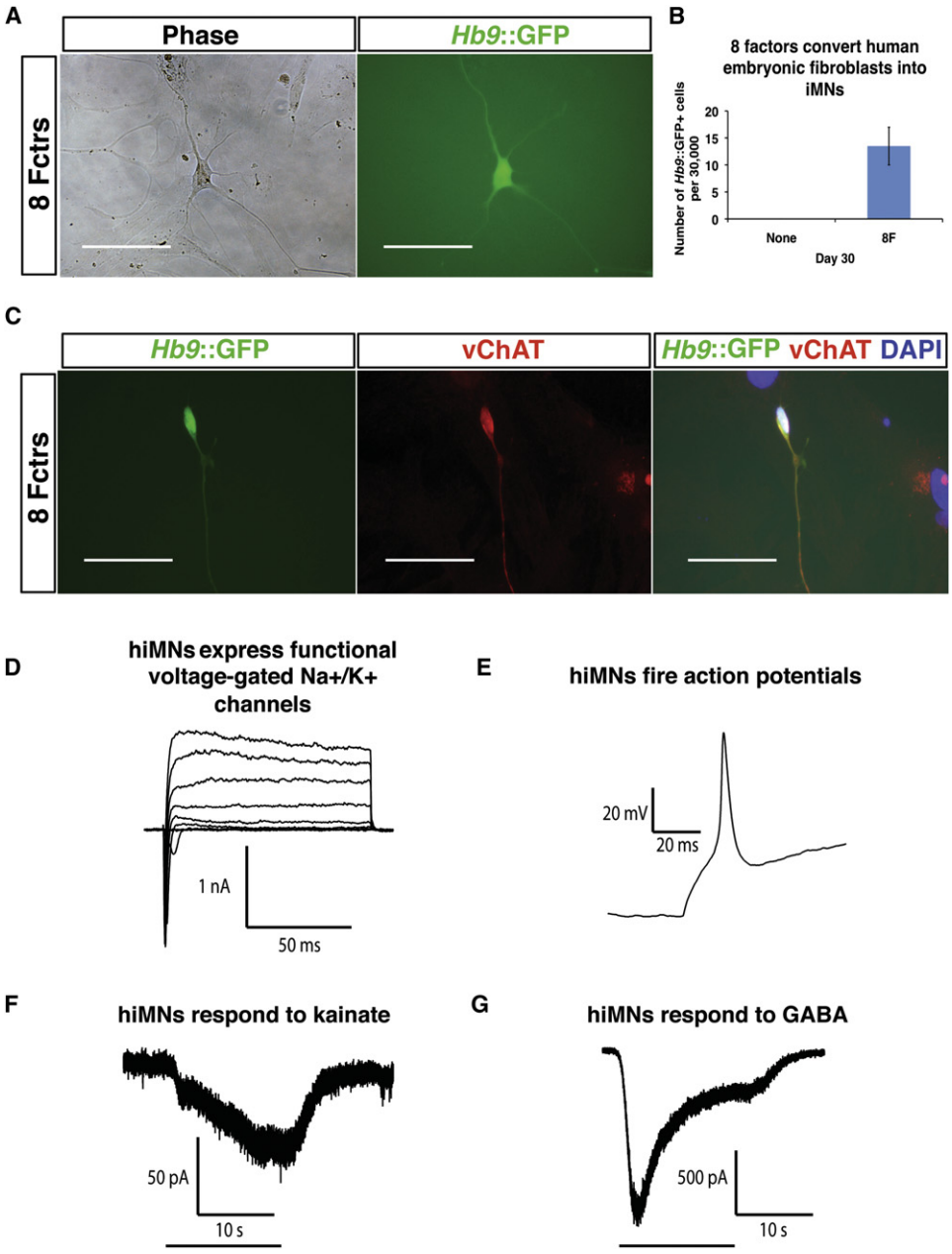

Figure 7. Human iMNs Are Generated by Eight Transcription Factors

(A) An *Hb9::*GFP+ neuron generated from a HEF culture by eight transcription factors. Scale bars represent 80 μm.
(B) Quantification of human iMN reprogramming efficiency at day 30 posttransduction. Error bars indicate ± SD.
(C) Human iMNs express vChAT (red). Scale bars represent 80 μm.
(D) Human iMNs express functional sodium and potassium channels.
(E) Human iMNs fire action potentials upon depolarization.
(F) One hundred micromolars of kainate induces inward currents in human iMNs.
(G) One hundred micromolars GABA induces inward currents in human iMNs.

EXPERIMENTAL PROCEDURES

Molecular Cloning, Isolating Embryonic and Adult Fibroblasts, Viral Transduction, and Cell Culture

Complementary DNAs for the 11 candidate factors were each cloned into the pMXs retroviral expression vector using Gateway technology (Invitrogen). *Hb9::*GFP-transgenic mice (Jackson Laboratories) were mated with ICR mice (Taconic) and MEFs were harvested from *Hb9::*GFP E12.5 embryos under a dissection microscope (Leica). Tail tip fibroblasts were isolated from *Hb9::*GFP-transgenic adult mice as previously described (Vierbuchen et al., 2010). The fibroblasts were passaged at least once before being used for experiments. HEFs were isolated from human ESCs by culturing them in DMEM + 20% fetal bovine serum without bFGF for at least three passages. Retroviral transduction was performed as described (Ichida et al., 2009). Glial

cells isolated from P2 ICR mouse pups were added to infected fibroblasts 2 days after transduction. The next day, medium was switched to either mouse motor neuron medium containing F-12 (Invitrogen), 5% horse serum, N2 and B27 supplements, glutamax and penicillin/streptomycin, or to N3 medium (Vierbuchen et al., 2010). Both media were supplemented with GDNF, BDNF, and CNTF, all at 10 ng/ml. Efficiency of iMN generation was estimated by counting the number of *Hb9::*GFP+ cells with neuronal morphologies using a fluorescence microscope (Nikon), and two-tailed Student's t test was used for statistical analysis.

Obtaining ESC-Derived and Embryonic Motor Neurons, FACS, Microarray Analysis, and qPCR

Motor neurons were derived from *Hb9::*GFP mouse ESCs and isolated by FACS using standard protocol (Di Giorgio et al., 2007). Embryonic motor neurons were harvested from *Hb9::*GFP E13.5 embryos. Briefly, whole spinal cords were washed in F-12 (Invitrogen) and incubated in 10 ml of 0.025% trypsin with DNase for 45 min with gentle agitation every 15 min. Media was added to the dissociated spinal cords and the cells were triturated, spun down at 1,000 rpm for 5 min, and resuspended in DMEM/F-12 with glutamax and penicillin/streptomycin. FACS was performed in the same way as with ESC-derived motor neurons. Total RNA isolation, RNA amplification, and microarray analysis were performed as described previously (Ichida et al., 2009). Gene expression data for mouse ESCs and MEFs (GEO accession: GSE18286) obtained in a previous study (Ichida et al., 2009) were also used for comparison. qPCR was performed using iScript cDNA Synthesis Kit and SYBR Green qPCR Supermix (Bio-Rad) according to manufacturers' instructions, with the primers in Table S1.

Immunocytochemistry

Antibody staining was performed as previously described (Ichida et al., 2009). The following primary antibodies were used: mouse anti-Hb9 (DSHB, 1:50); mouse anti-Islet (DSHB, 1:100); mouse anti-TuJ1 (Covance, 1:500); rabbit anti-vChAT (Sigma, 1:1,000); rabbit anti-synapsin I (Millipore, 1:500); and rabbit anti-tyrosine hydroxylase (ThermoScientific, 1:300).

Electrophysiology

Whole-cell voltage-clamp and current-clamp recordings were made using a Multiclamp 700B (Molecular Devices) at room temperature (21°C–23°C). Data were digitized with a Digidata 1440A A/D interface and recorded using pCLAMP 10 software (Molecular Devices). Data were low-pass filtered at 2 kHz and sampled at 20 kHz (1 kHz and 2 kHz, respectively, for transmitter application). Patch pipettes were pulled from borosilicate glass capillaries on a Sutter Instruments P-97 puller and had resistances of 2–4 MΩ. The pipette capacitance was reduced by wrapping the shank with Parafilm and compensated for using the amplifier circuitry. Series resistance was typically 5–10 MΩ, always less than 15 MΩ, and compensated by at least 80%. Leak currents were typically less than 200 pA with a mean input resistance of 675 MΩ and a mean resting potential −49 mV. For study of voltage-gated conductances, linear leakage currents were digitally subtracted using a P/4 protocol and voltage was stepped from a holding potential of −80 mV to test potentials from −80 to 30 mV in 10 mV increments. Intracellular solutions were potassium-based solution and contained, in mM, KCl, 150; $MgCl_2$, 2; and HEPES, 10 (pH 7.4) for earlier experiments and KCl, 135; $MgCl_2$, 2; HEPES, 10; MgATP, 4; NaGTP, 0.3; Na_2PhosCr, 10; and EGTA, 1 (pH 7.4) for later experiments, with no obvious difference in sodium and potassium currents. The extracellular solution was sodium-based and contained, in mM, NaCl, 135; KCl, 5; $CaCl_2$, 2; $MgCl_2$, 1; glucose, 10; and HEPES, 10 (pH 7.4). Based on the chloride Nernst potential of −2 mV, inward currents were expected following GABA and glycine treatment (Puia et al., 1990). Transmitters were not washed out, explaining the delayed current decay.

C2C12 Muscle Coculture

C2C12 myoblasts were expanded in DMEM with 20% fetal bovine serum and penicillin/streptomycin. When the culture reached 100% confluency, the serum content was reduced to 5% to induce differentiation. Flow-purified iMNs or iNs were added to the myotubes after 7–14 days and the medium switched to either mouse motor neuron or N3 media. The cocultures were monitored for myotube contractions under the microscope with 10× or 20× objectives. To stop contractions, a solution of tubocurarine hydrochloride was added to a final concentration of between 50 nM and 50 μM. Twitching myotubes were filmed using Nikon ACT-2U Imaging Software (Excel Technologies) and contraction frequencies were determined.

iMN-Chick Myotube Cocultures and Immunocytochemistry

Myoblasts were isolated from the epaxial (longissimus) muscles of E10 White Leghorn chick embryos and plated in 24-well plates at a density of 100,000 cells/well. Cultures were maintained at 37°C in F10 media (GIBCO) supplemented with 0.44 mg/ml calcium chloride, 10% horse serum, 5% chicken serum, and 2% penicillin/streptomycin. iMNs were added to the myotubes 5 days later in Neurobasal media (GIBCO) supplemented with B27 (GIBCO), 1% L-glutamine, and 1% penicillin:streptomycin. Cocultures were supplemented with 10 ng/ml CNTF and GDNF every 2 days for the first week following the addition of the iMNs. Cocultures were maintained for 3 weeks when they were prepared for immunocytochemistry. Antibody staining was performed as previously described (Soundararajan et al., 2006). A rabbit anti-GFP (Chemicon, 1:2,000) primary antibody was used to visualize the iMNs, and rhodamine-conjugated α-BTX (Invitrogen, 1:500) was used to visualize the ACh receptors. Images were acquired on a laser scanning-confocal microscope (Zeiss LSM 510). Orthogonal images were rendered and edited with LSM imaging software (Zeiss) and further contrast and brightness adjustments were performed in Photoshop version 7.0.

In Ovo Transplantation of ESC-Derived Motor Neurons and iMNs

In ovo transplantations and immunohistochemistry were performed as previously described (Soundararajan et al., 2006). Briefly, E2.5 chick embryos were exposed; the vitelline membrane and amnion were cut to allow surgical access to the neural tube. An incision of 1–1.5 somites in length was made along the midline of the neural tube at the rostral extent of the developing hind limb bud (T7-L1) using a flame-sterilized tungsten needle (0.077 mm wire, World Precision Instruments). For control ESC-derived motor neuron transplantations, *Hb9::*GFP-transgenic mouse ESCs were differentiated into motor neurons as described previously (Soundararajan et al., 2006; Wichterle et al., 2002). A single embryoid body containing approximately 150–200 differentiated *Hb9::*GFP+ motor neurons was transplanted into the ventral lumen of the neural tube of E2.5 chick embryos as described previously (Soundararajan et al., 2006). For iMN transplantations, a sphere of iMNs mixed with nontransgenic, ESC-derived motor neurons containing approximately 200 cells was transplanted into the ventral lumen of the neural tube of E2.5 chick embryos. For all transplantations, the chick embryos were harvested 5 days later, fixed in 4% paraformaldehyde/PBS, cut on a cryostat, and then processed for immunohistochemistry. The following primary antibodies were used: rabbit anti-GFP (Chemicon, 1:1,000) and mouse anti-Tuj1 (Covance, 1:1,000). Images were captured with a digital camera (C4742; Hamamatsu Photonics, Hamamatsu, Japan) in conjunction with digital imaging acquisition software (IPLab; Version 4.0; BD Biosciences, Rockville, MD).

Glia-Neuron Coculture for Disease Modeling

*SOD1*G93A transgenic mice (Jackson Laboratories) were mated with ICR mice. Glial preps were derived from transgenic P2 pups and their littermates. Three weeks later, confluent flasks of glial cells were passaged 1:2 onto six-well plates and iMNs were plated on top. The cocultures were kept in mouse motor neuron medium with neurotrophic factors and the media changed every other day for the duration of the experiment. Two-tailed Student's t test was used for statistical analysis.

Nestin::CreER Lineage Tracing

MEFs were isolated from E13.5 embryos that were transgenic for *Nestin*::CreER, LOX-STOP-LOX-H2B-mCherry, and *Hb9*::GFP. To generate iPSCs, the MEFs were transduced with retroviruses (pMXs vector) encoding *Oct4*, *Sox2*, and *Klf4*. Cells were cultured in mouse ESC media containing 13% Knockout Serum Replacement, and colonies were picked, expanded, and verified by Nanog immunostaining. For the positive control, iPSCs were differentiated into motor neurons using retinoic acid and Sonic Hedgehog

(Wichterle et al., 2002) in the presence or absence of 1–2 μM 4-OHT. iMNs were also created in the presence or absence of 2 μM 4-OHT.

ACCESSION NUMBERS

Microarray data have been submitted to the GEO repository with accession number GSE31160.

SUPPLEMENTAL INFORMATION

Supplemental Information for this article includes four figures, two tables, and one movie, and can be found with this article online at doi:10.1016/j.stem.2011.07.014.

ACKNOWLEDGMENTS

We are grateful to A.C. Carter for help with lineage tracing experiments and E. Kiskinis, S. de Boer, G. Boulting, and J. Rivera-Feliciano for providing reagents and helpful discussions. We would also like to thank B. Tilton for assistance with FACS, K. Harrison for providing the mouse *Hb9* cDNA, N. Atwater for assistance with glia preparation, J. Sandoe and K. Sandor for help with molecular cloning, K. Koszka for help with mouse husbandry, and M.Y. Son for help with the diagram in Figure 1. This work was made possible by support provided by the Howard Hughes Medical Institute, the Harvard Stem Cell Institute, P^2ALS, the New York Stem Cell Foundation, NIH GO grant 1RC2 NS069395-01, and NIH grant R01 HD045732-03 to K.E. J.K.I. is supported by the Novartis Institutes for BioMedical Research and a Stan and Fiona Druckenmiller/New York Stem Cell Foundation postdoctoral fellowship. B.J.W. is supported by NIH Training Grant 5T32GM007592. C.J.W. used facilities provided by the Children's Hospital Boston Intellectual and Developmental Disabilities Research Center and the NIH. J.S.T. was funded by a Natural Sciences and Engineering Research Council of Canada graduate student scholarship award. V.F.R is supported by the Natural Sciences and Engineering Research Council of Canada. The authors are filing a patent based on the results reported in this paper. K.E. is a member of the iPierian scientific advisory board.

Received: June 29, 2011
Revised: July 22, 2011
Accepted: July 29, 2011
Published online: August 18, 2011

REFERENCES

Abe, T., Kiyonari, H., Shioi, G., Inoue, K., Nakao, K., Aizawa, S., and Fujimori, T. (2011). Establishment of conditional reporter mouse lines at ROSA26 locus for live cell imaging. Genesis *49*, 579–590.

Alessandri-Haber, N., Paillart, C., Arsac, C., Gola, M., Couraud, F., and Crest, M. (1999). Specific distribution of sodium channels in axons of rat embryo spinal motoneurones. J. Physiol. *518*, 203–214.

Burns, K.A., Ayoub, A.E., Breunig, J.J., Adhami, F., Weng, W.L., Colbert, M.C., Rakic, P., and Kuan, C.Y. (2007). Nestin-CreER mice reveal DNA synthesis by nonapoptotic neurons following cerebral ischemia hypoxia. Cereb. Cortex *17*, 2585–2592.

Caiazzo, M., Dell'anno, M.T., Dvoretskova, E., Lazarevic, D., Taverna, S., Leo, D., Sotnikova, T.D., Menegon, A., Roncaglia, P., Colciago, G., et al. (2011). Direct generation of functional dopaminergic neurons from mouse and human fibroblasts. Nature, in press. Published online July 3, 2011. 10.1038/nature10284.

Cui, D., Dougherty, K.J., Machacek, D.W., Sawchuk, M., Hochman, S., and Baro, D.J. (2006). Divergence between motoneurons: gene expression profiling provides a molecular characterization of functionally discrete somatic and autonomic motoneurons. Physiol. Genomics *24*, 276–289.

Dahm, L.M., and Landmesser, L.T. (1988). The regulation of intramuscular nerve branching during normal development and following activity blockade. Dev. Biol. *130*, 621–644.

Di Giorgio, F.P., Carrasco, M.A., Siao, M.C., Maniatis, T., and Eggan, K. (2007). Non-cell autonomous effect of glia on motor neurons in an embryonic stem cell-based ALS model. Nat. Neurosci. *10*, 608–614.

Di Giorgio, F.P., Boulting, G.L., Bobrowicz, S., and Eggan, K.C. (2008). Human embryonic stem cell-derived motor neurons are sensitive to the toxic effect of glial cells carrying an ALS-causing mutation. Cell Stem Cell *3*, 637–648.

Frederiksen, K., and McKay, R.D. (1988). Proliferation and differentiation of rat neuroepithelial precursor cells in vivo. J. Neurosci. *8*, 1144–1151.

Ichida, J.K., Blanchard, J., Lam, K., Son, E.Y., Chung, J.E., Egli, D., Loh, K.M., Carter, A.C., Di Giorgio, F.P., Koszka, K., et al. (2009). A small-molecule inhibitor of tgf-Beta signaling replaces sox2 in reprogramming by inducing nanog. Cell Stem Cell *5*, 491–503.

Ieda, M., Fu, J.D., Delgado-Olguin, P., Vedantham, V., Hayashi, Y., Bruneau, B.G., and Srivastava, D. (2010). Direct reprogramming of fibroblasts into functional cardiomyocytes by defined factors. Cell *142*, 375–386.

Jessell, T.M. (2000). Neuronal specification in the spinal cord: inductive signals and transcriptional codes. Nat. Rev. Genet. *1*, 20–29.

Lee, S.K., Lee, B., Ruiz, E.C., and Pfaff, S.L. (2005). Olig2 and Ngn2 function in opposition to modulate gene expression in motor neuron progenitor cells. Genes Dev. *19*, 282–294.

Lupa, M.T., and Hall, Z.W. (1989). Progressive restriction of synaptic vesicle protein to the nerve terminal during development of the neuromuscular junction. J. Neurosci. *9*, 3937–3945.

Messam, C.A., Hou, J., Berman, J.W., and Major, E.O. (2002). Analysis of the temporal expression of nestin in human fetal brain derived neuronal and glial progenitor cells. Brain Res. Dev. Brain Res. *134*, 87–92.

Miles, G.B., Yohn, D.C., Wichterle, H., Jessell, T.M., Rafuse, V.F., and Brownstone, R.M. (2004). Functional properties of motoneurons derived from mouse embryonic stem cells. J. Neurosci. *24*, 7848–7858.

Nagai, M., Re, D.B., Nagata, T., Chalazonitis, A., Jessell, T.M., Wichterle, H., and Przedborski, S. (2007). Astrocytes expressing ALS-linked mutated SOD1 release factors selectively toxic to motor neurons. Nat. Neurosci. *10*, 615–622.

Pang, Z.P., Yang, N., Vierbuchen, T., Ostermeier, A., Fuentes, D.R., Yang, T.Q., Citri, A., Sebastiano, V., Marro, S., Sudhof, T.C., et al. (2011). Induction of human neuronal cells by defined transcription factors. Nature, in press. Published online May 26, 2011. 10.1038/nature10202.

Peljto, M., and Wichterle, H. (2011). Programming embryonic stem cells to neuronal subtypes. Curr. Opin. Neurobiol. *21*, 43–51.

Peljto, M., Dasen, J.S., Mazzoni, E.O., Jessell, T.M., and Wichterle, H. (2010). Functional diversity of ESC-derived motor neuron subtypes revealed through intraspinal transplantation. Cell Stem Cell *7*, 355–366.

Pfisterer, U., Kirkeby, A., Torper, O., Wood, J., Nelander, J., Dufour, A., Björklund, A., Lindvall, O., Jakobsson, J., and Parmar, M. (2011). Direct conversion of human fibroblasts to dopaminergic neurons. Proc. Natl. Acad. Sci. USA *108*, 10343–10348.

Puia, G., Santi, M.R., Vicini, S., Pritchett, D.B., Purdy, R.H., Paul, S.M., Seeburg, P.H., and Costa, E. (1990). Neurosteroids act on recombinant human GABAA receptors. Neuron *4*, 759–765.

Soundararajan, P., Miles, G.B., Rubin, L.L., Brownstone, R.M., and Rafuse, V.F. (2006). Motoneurons derived from embryonic stem cells express transcription factors and develop phenotypes characteristic of medial motor column neurons. J. Neurosci. *26*, 3256–3268.

Soundararajan, P., Lindsey, B.W., Leopold, C., and Rafuse, V.F. (2007). Easy and rapid differentiation of embryonic stem cells into functional motoneurons using sonic hedgehog-producing cells. Stem Cells *25*, 1697–1706.

Soundararajan, P., Fawcett, J.P., and Rafuse, V.F. (2010). Guidance of postural motoneurons requires MAPK/ERK signaling downstream of fibroblast growth factor receptor 1. J. Neurosci. *30*, 6595–6606.

Szabo, E., Rampalli, S., Risueño, R.M., Schnerch, A., Mitchell, R., Fiebig-Comyn, A., Levadoux-Martin, M., and Bhatia, M. (2010). Direct conversion of human fibroblasts to multilineage blood progenitors. Nature *468*, 521–526.

Takahashi, K., and Yamanaka, S. (2006). Induction of pluripotent stem cells from mouse embryonic and adult fibroblast cultures by defined factors. Cell *126*, 663–676.

Vierbuchen, T., Ostermeier, A., Pang, Z.P., Kokubu, Y., Südhof, T.C., and Wernig, M. (2010). Direct conversion of fibroblasts to functional neurons by defined factors. Nature *463*, 1035–1041.

Wichterle, H., Lieberam, I., Porter, J.A., and Jessell, T.M. (2002). Directed differentiation of embryonic stem cells into motor neurons. Cell *110*, 385–397.